Supplementary Information

The Covalent Functionalization of Few-layered MoTe2 Thin Films with Iodonium Salts

Olga Guselnikova,[a] * James P. Fraser,[b] Natalia Soldatova,[a] Elizaveta Sviridova, [a] Alexey Ivanov,[a] Raul Rodriguez,[a] Alexey Y. Ganin,[b,*] Pavel Postnikov[a,*]

a) *Research School of Chemistry and Applied Biomedical Sciences, Tomsk Polytechnic University, Tomsk 634050, Russian Federation*

b) *International Center for Materials Nanoarchitechtonics (MANA) and International Center for Young Scientists (ICYS), National Institute for Materials Science (NIMS), 1-1 Namiki, Tsukuba, Ibaraki 305-0044, Japan*

b) *School of Chemistry, University of Glasgow, Glasgow, G12 8QQ, United Kingdom*

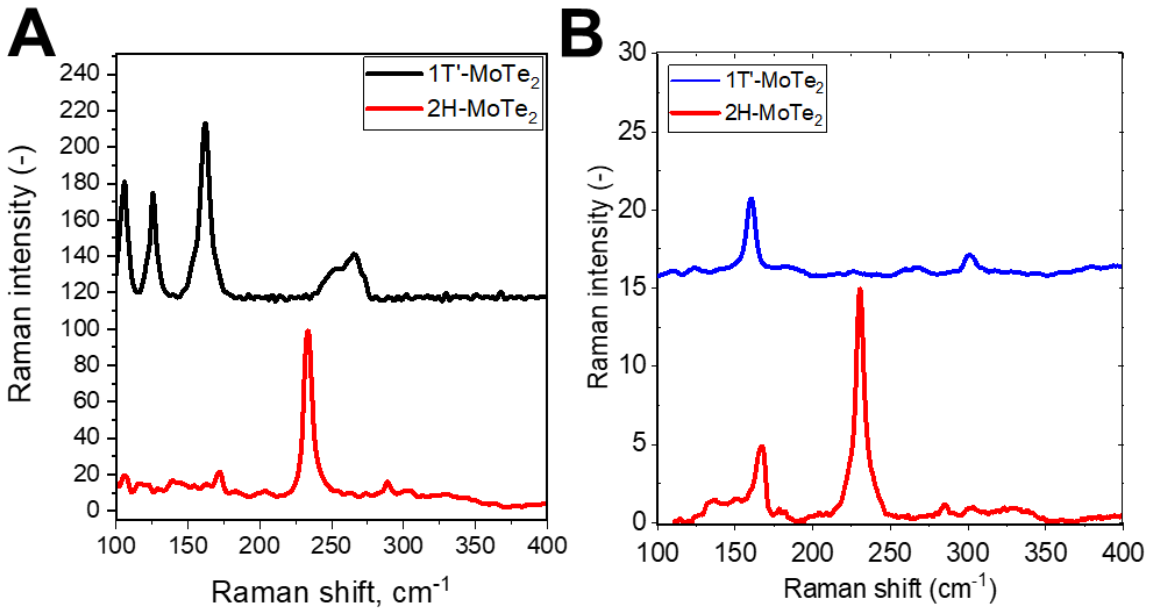

Figure S1. Raman spectra of pristine, non-functionalized 1T'-$MoTe_2$ and 2H-$MoTe_2$ thin films on 300 nm SiO_2/Si substrates collected with 532 nm (**A**) and 633 nm lasers (**B**).

Table S1A. Wavenumbers of the characteristic Raman modes of 1T'-$MoTe_2$ before and after functionalization with **IS-CF_3** using 532 nm and 633 nm lasers.

	E1g		**A1g**		**E2g**		**B2g**		**Others**	
	633	532	633	532	633	532	633	532		
1T-$MoTe_2$	110±1	105.8±1	**126.2±1**	**125.7±1**	161±1	162.3±1	186±1	N/A	267±1	264. ±18
1T'- $MoTe_2$-CF_3	108±1	104.7±1	**123±1**	**124.8±1**	160±1	162.7±1	184±1	N/A	267±1	266.2±1

Table S1B. Wavenumbers of the characteristic Raman modes of 2H-$MoTe_2$ before and after functionalization with **IS-CF_3** using 532 nm and 633 nm lasers.

	E1g		**A1g**		**E2g**		**B2g**	
	633	532	633	532	633	532	633	532
Pristine 2H	114±1	106	**167.3±1**	**172±1**	230.1±1	233.5	285.1±1	289±1
2H- $MoTe_2$-CF_3	113±1	104.5	**165.5±1**	**169±1**	230±1	233.1	285.1±1	287.8±1

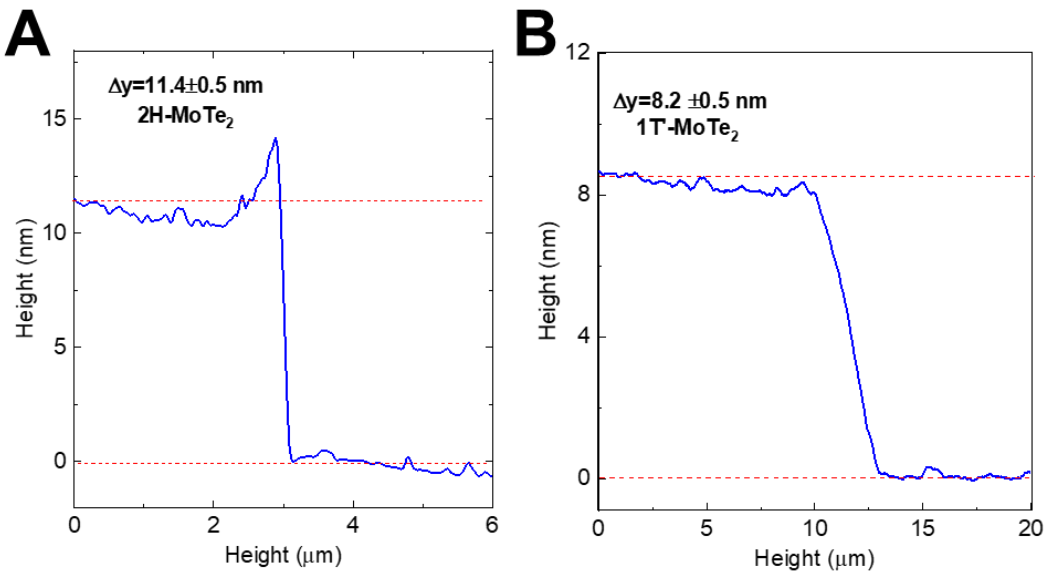

Figure S2. Height profiles obtained from AFM measurements on pristine, non-functionalized 2H-$MoTe_2$ (**A**) and 1T'-$MoTe_2$ (**B**) thin films on 300 nm SiO_2/Si substrates.

XPS characterization of pristine films

Contrary to Raman spectroscopy, which suggested that no oxide impurities were present in the samples, the analysis of XPS survey spectra showed the presence of oxygen (Fig. S3). High-resolution XPS analysis of Mo 3d and Te 3d showed the presence of oxidized states on the surface, typical for $MoTe_2$ films exposed to the ambient environment.[1] Apart from the expected peaks associated with Mo – Te bonds, high-resolution Mo 3d spectra (Fig. S4) show distinctive shoulders at binding energies (BE) of about 232.4 eV and 235.4 eV corresponding to Mo – O bonds.[1] Similarly, along with peaks associated with Te – Mo bonding, the presence of a Te – O is also confirmed in the high-resolution Te 3d spectra at BE around 576.3 eV and 586.3 eV (Fig. S4). The positions of observed peaks (Table S2) are consistent with the reported XPS values on $MoTe_2$ films exposed to the ambient.[1] The XPS results highlight the low sensitivity of Raman spectroscopy as a characterization method for detection of surface oxides. It appears to be insensitive to $MoTeO_x$ formed at the surface of the films.

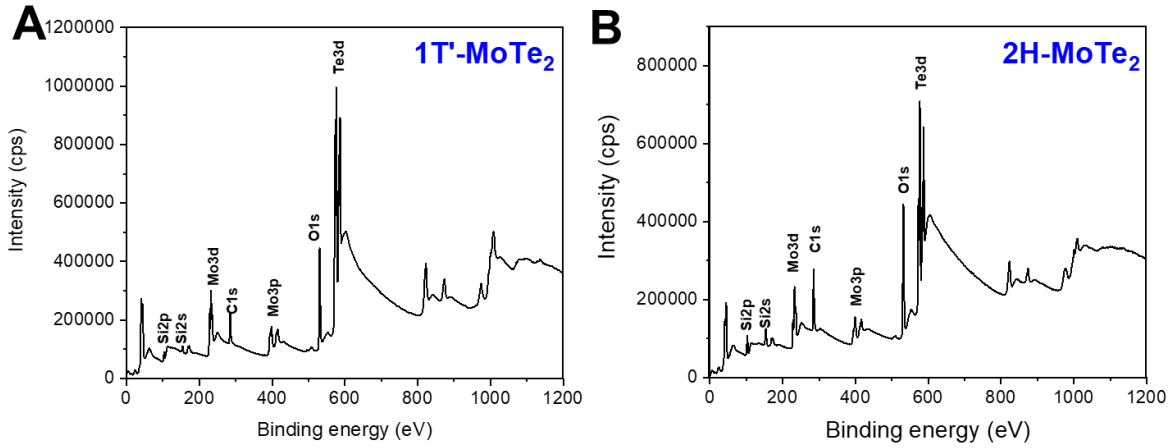

Figure S3. XPS survey spectra from pristine, non-functionalized 1T'-$MoTe_2$ (**A**) and 2H-$MoTe_2$ (**B**) thin films on 300 nm SiO_2/Si substrates.

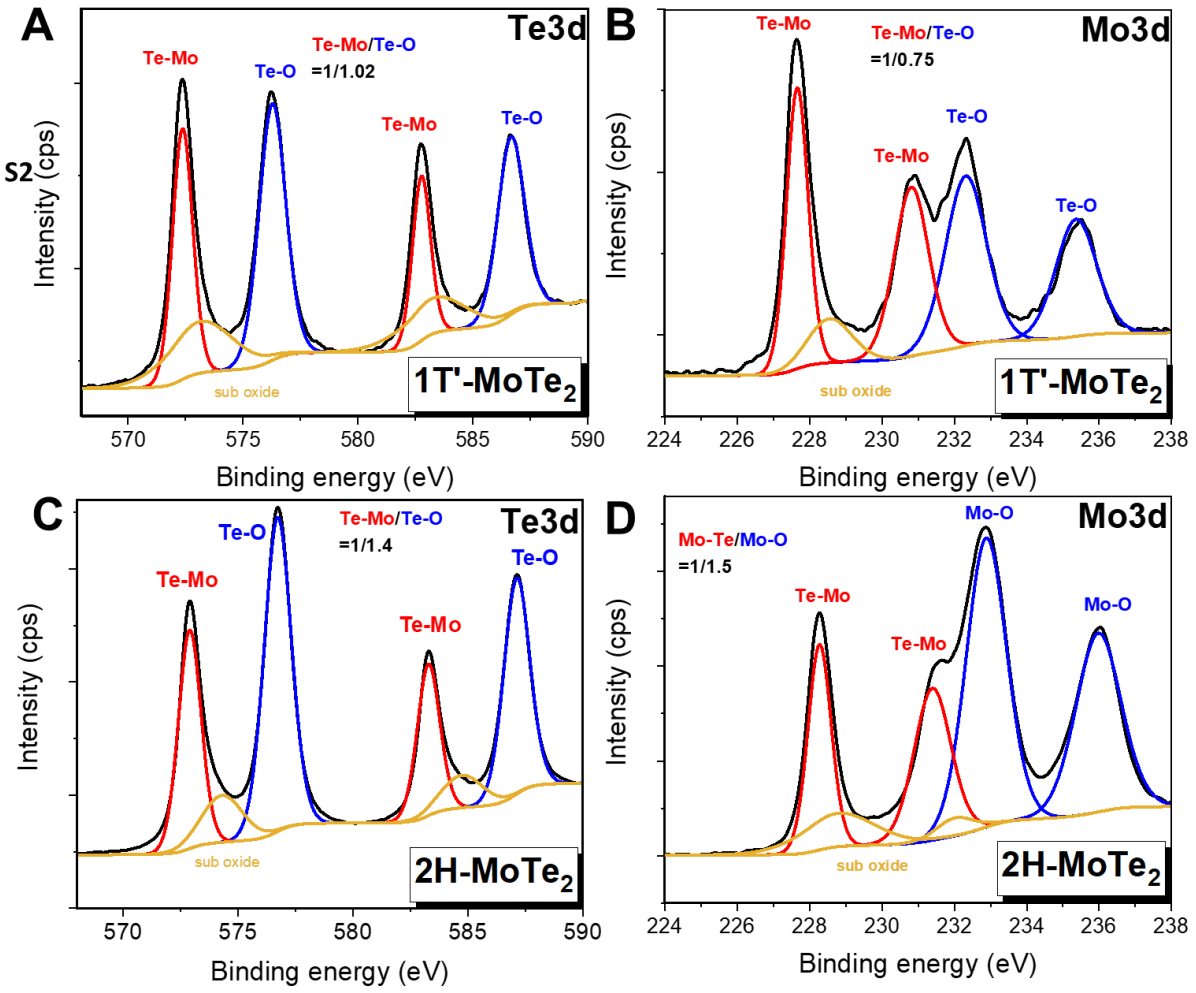

Figure S4. High resolution XPS spectra for Te 3d and Mo 3d regions collected from pristine, non-functionalized 1T'-$MoTe_2$ (**A, B**) and 2H-$MoTe_2$ (**C, D**) films on 300 nm SiO_2/Si substrates. The experimentally obtained spectra are shown in black whilst the red, blue and yellow solid lines are simulated profiles for the relevant peaks.

Table S2. The positions of Mo 3d and Te3d peaks from high resolution XPS spectra collected from the respective films before and after functionalization with **IS-CF_3**.

Peak position	**1T-$MoTe_2$**	**1T-$MoTe_2$-CF_3**	**2H-$MoTe_2$**	**2H-$MoTe_2$-CF_3**
Mo $3d_{5/2}$	227.68	227.83	228.25	228.37
Mo $3d_{5/2}$ [ox]	232.35	232.34	232.9	233.0
Mo $3d_{3/2}$	230.09	230.96	231.4	231.56
Mo $3d_{5/2}$ [ox]	235.41	235.41	235.97	236.0
Te $3d_{5/2}$	572.48	572.88	572.8	573.04
Te-C	-	573.37	-	573.78
Te $3d_{5/2}$ [ox]	573.21	573.26	576.82	574.94
Te $3d_{3/2}$	582.85	583.28	583.3	583.48
Te-C	-	583.53	-	584.2
Te $3d_{5/2}$ [ox]	583.46	583.24	587.23	587.1

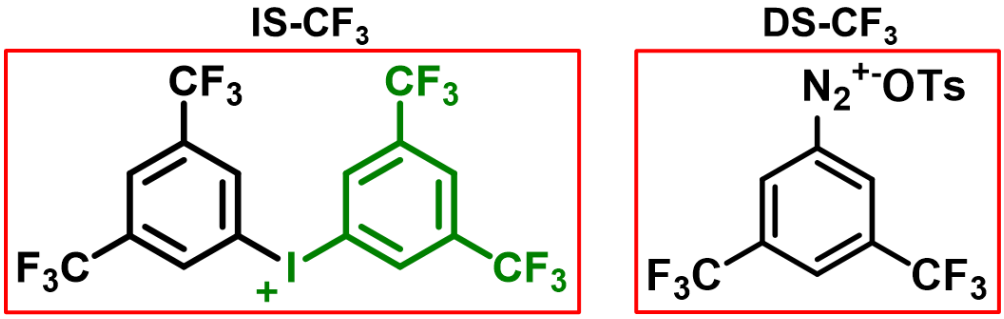

Figure S5. Chemical structure of (3,5-bis(trifluoromethyl)phenyl)iodonium trifluoromethanesulfonate **(IS-CF_3)** and 3,5-bis(trifluoromethyl)benzenediazonium tosylate (**DS-CF_3**).

Testing interactions with solvents

As solvents may take part in the reaction or lead to degradation of the surface, it was important to run an experiment with them as a control sample. Therefore, before the experiments with **IS-CF3**, the stability of $MoTe_2$ was tested in degassed MeOH : CH_3CN. The $MoTe_2$ films showed no evident changes according to Raman spectroscopy before and after immersion of the films into the solvent for 1 hour (Fig. S6). In addition, survey XPS spectra showed only negligible differences between the initial film and the film after solvent immersion (Fig. S7).

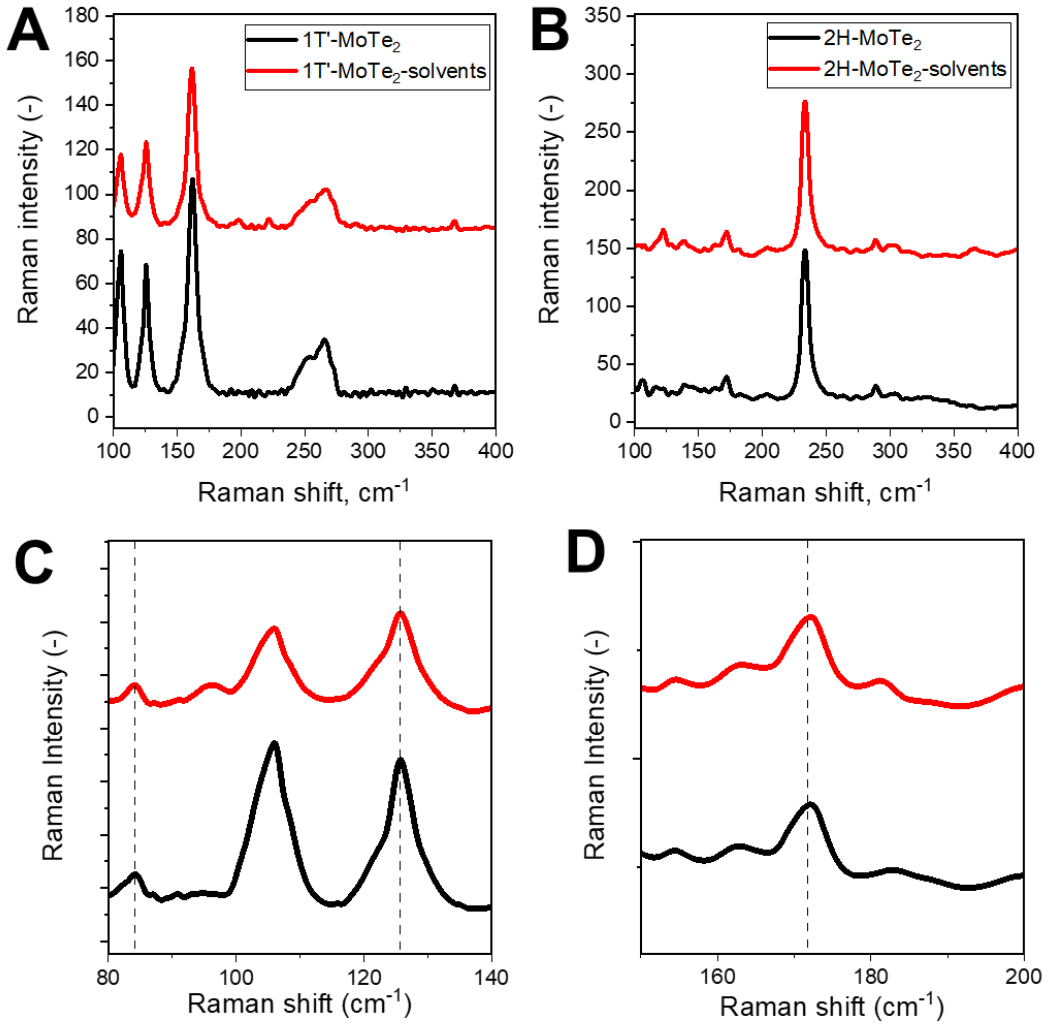

Figure S6. Raman spectra (532 nm) obtained from 1T'-$MoTe_2$ (**A**) and 2H-$MoTe_2$ (**B**) films before (black solid line) and after (red solid line) immersion in a solution of 50 % MeOH : 50 % CH_3CN for 1 hour. The zoom regions for the most intense peak are shown in **C** and **D**.

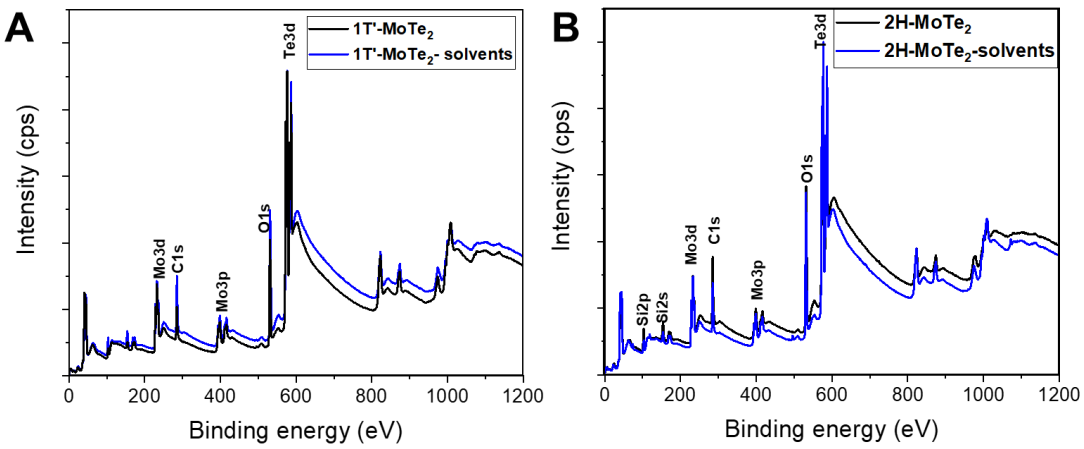

Figure S7. XPS survey spectra of 1T'-$MoTe_2$ (**A**) and 2H-$MoTe_2$ (**B**) films obtained before (black solid line) and after (blue solid line) immersion in a solution of 50 % MeOH : 50 % CH_3CN for 1 hour.

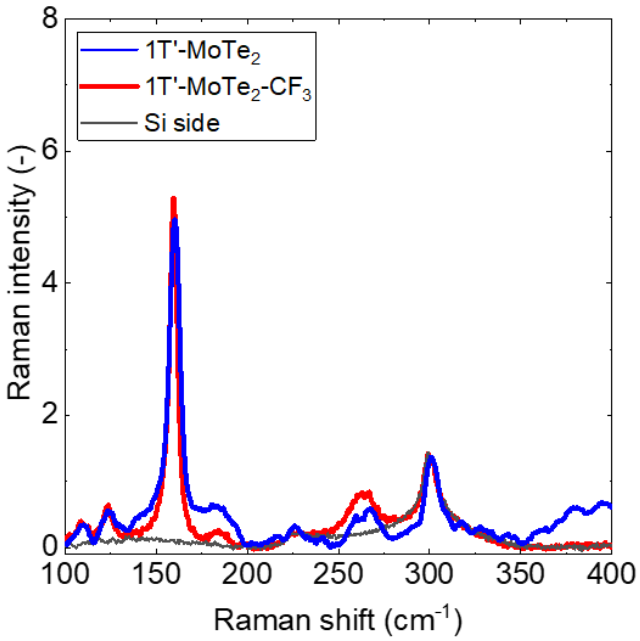

Figure S8. Raman spectra of 1T'-$MoTe_2$ and 1T'-$MoTe_2$-CF_3 using 633 nm laser.

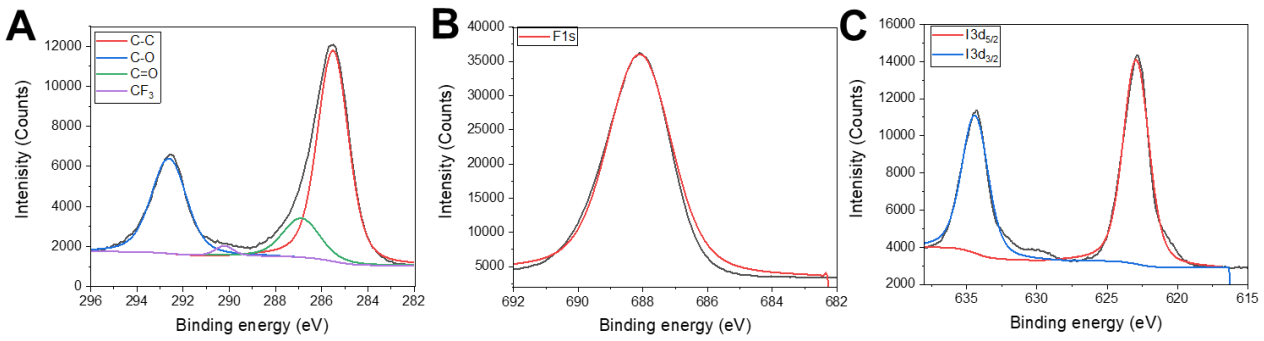

Figure S9. High resolution C 1s (**A**), F1s (**B**) and I 3d (**C**) XPS spectra collected on pristine bis(3,5-bis(trifluoromethyl)phenyl)iodonium trifluoromethanesulfonate immobilized as powder on Cu tape.

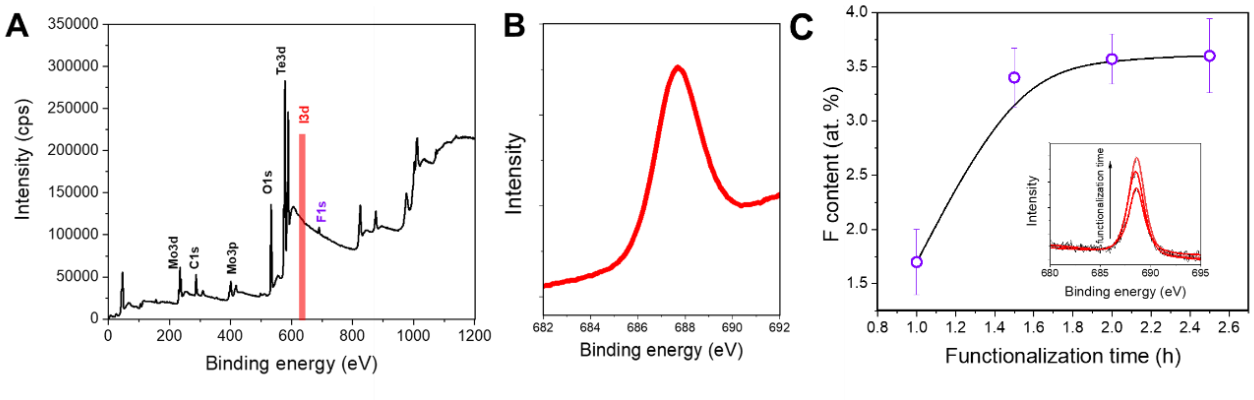

Figure S10. (**A**) XPS survey spectra of 1T'-$MoTe_2$-CF_3 with the absence of I 3d peak highlighted, (**B**) the overlap of all spectra collected on F 1s peak on Fig. 2G and (**C**) Dependence of F content in atomic % on the functionalization time

Supplementary Note 1

Calculation of the aryl adlayer thickness from the attenuation of XPS Te $3d_{5/2}$ peak.

The thickness of organic adlayer can be estimated based on the attenuation of XPS peak intensities before and after functionalization. Following the method described in[2] the attenuation of Te signal from Te $3d_{5/2}$ (572.48 eV for 1T'- and 572.8 eV for 2H-$MoTe_2$) due to attachment of functional group was selected to calculate the thickness of the organic adlayer using the following equation:

$I / I_0 = \exp(-d / \lambda \sin\theta)$

d - organic layer thickness in nm

λ - mean free path of the substrate-specific photoelectron in the organic layer in mg m^{-2}

θ - the take-off angle to the surface (90° in our case)

I / I_0- ratio of the Te $3d_{5/2}$ peak intensities (I_0 - before and I - after modification)

The value of λ can be deducted from the empirical formula derived by Seah and Dench[3]

$\lambda = A_n / E_k^2 + B_n E_k^{1/2}$

For a substrate covered with an organic material $A_n = 49$ and $B_n = 0.11$.[2] E_k is the kinetic energy of photoelectrons for the Al K_α source E_k = 1486.6 eV – BE, where BE is the binding energy of the relevant Te 3d peaks (which correspond to 572.48 eV in 1T'-$MoTe_2$ and 572.8 eV in 2H-$MoTe_2$). Since the unit of λ in this formula is in nm, it should be converted into λ (mg m^{-2}) by taking into account the density of 1.3 g cm^{-3} of 1,3-Bis(trifluoromethyl)benzene.

Using the equation for $d = -\lambda \sin\theta \ln(I / I_0)$ the aryl adlayer thicknesses are:

d = 1.3±0.8 nm for **1T'-$MoTe_2$**

d = 2.1±0.9 nm for **2H-$MoTe_2$**

Calculation of the density of grafted Ar-$(CF_3)_2$

The surface coverage (Γ, in molecules cm^{-2}) of **1T'-$MoTe_2$** with Ar-$(CF_3)_2$ was calculated:

$\Gamma\ (Ar(CF_3)_2) = [(N_A \times r \times d)/M] = [(6.02\ 10^{23}\ \text{molecules mol}^{-1} \times 1.3\ \text{g cm}^{-3} \times 1.3\ 10^{-7}\ \text{cm}) / 2.13\ 10^2\ \text{g mol}^{-1}] = 4.77\ 10^{14}\ \text{molecules cm}^{-2}$

where N_A – Avagadro number, ρ – density of organic layer, d – thickness of organic layer, M – molar mass of organic layer.

for **2H-$MoTe_2$:**

$\Gamma\ (Ar(CF_3)_2) = [(N_A \times r \times d)/M] = [(6.02\ 10^{23}\ \text{molecules mol}^{-1} \times 1.3\ \text{g cm}^{-3} \times 2.1\ 10^{-7}\ \text{cm}) / 2.13\ 10^2\ \text{g mol}^{-1}] = 7.71\ 10^{14}\ \text{molecules cm}^{-2}$

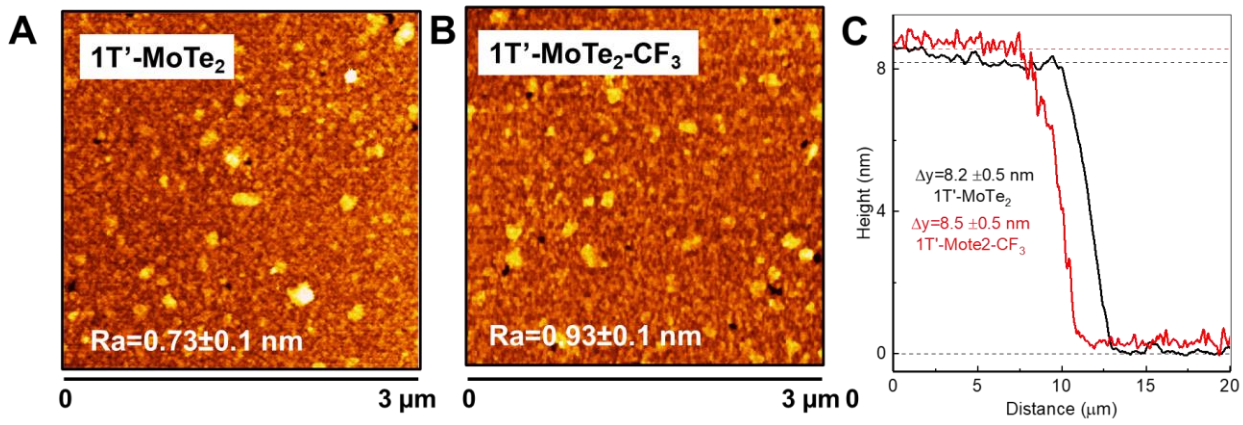

Figure S11. 2D topographical images obtained using AFM from 1T'-$MoTe_2$ (**A**) and 1T'-$MoTe_2$-CF_3 (**B**) and their corresponding height profiles (**C**).

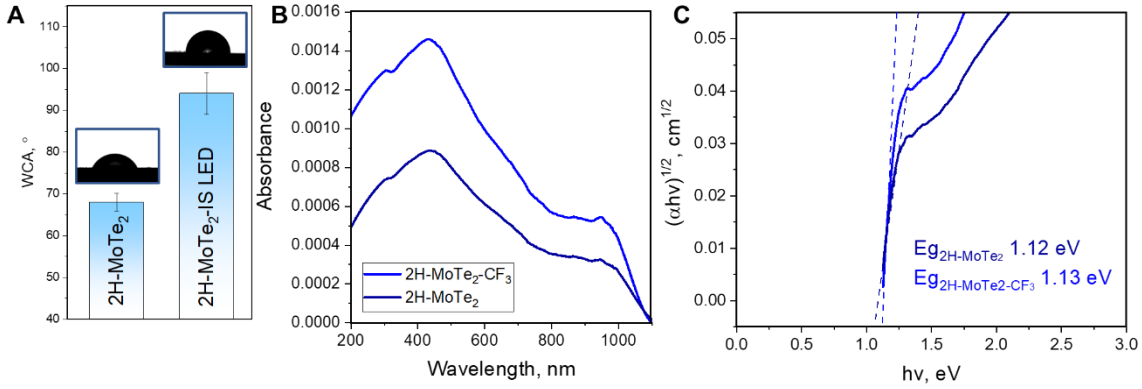

Figure 12. WCA measurements (**A**) and Tauc plot (**B**) for 1T'-$MoTe_2$ and 1T'-$MoTe_2$-CF_3.

Figures S12B and S21B displays the optical spectra of 1T'-$MoTe_2$ and 2H-$MoTe_2$ on quartz substrates before and after functionalization. Several peaks are clearly observable in the spectra of Figure 2a, which we have labeled according to the bulk assignments of Wilson and Yoffe.[4,5]. The optical spectra of functionalized $MoTe_2$ films demonstrate the higher absorbance compared to initial thin films. These spectroscopic features are associated with transitions in different parts of the Brillouin zone of $MoTe_2$. The B and A′, B′ are identified as excitonic transitions. the C and

D features have been attributed to regions of parallel bands near the Brillouin zone of $MoTe_2$[6] and to similar parallel bands in monolayers of other TMD materials.

Supplementary Note 2

Functionalization of $MoTe_2$ with diazonium salt (DS-CF_3)

Following a previous report on aromatic diazonium salts as modification agents for $MoTe_2$ flakes obtained by mechanical exfoliation[7] we attempted the chemical functionalization of 1T'-$MoTe_2$. In our case, we functionalized the 1T'-$MoTe_2$ film using 1 mM solution of (bis(3,5-bis(trifluoromethyl)benzenediazonium tosylate (**DS-CF_3**) in MeOH/CH_3CN. However, according to Raman and XPS results (Fig. S13A-C, Supplementary Note 2) there is no evidence for the presence of the 1T'-$MoTe_2$ film at the substrate after immersion into ADS solution. We could not determine whether the reaction with **DS-CF_3** leads to dissolution or delamination of the film from the substrate (Fig. S13D, E). However, as far as the functionalization experiments are concerned, we did not find any product at the substrate after the reaction. Therefore, we concluded that the high reactivity of **DS-CF_3** very likely makes it an unsuitable reaction agent for the functionalization of $MoTe_2$ thin films. This may explain the complete lack of literature data on covalent functionalization of $MoTe_2$ thin films currently, despite the popularity of diazonium salts as highly effective functionalization agents for other chalcogenides.[8]

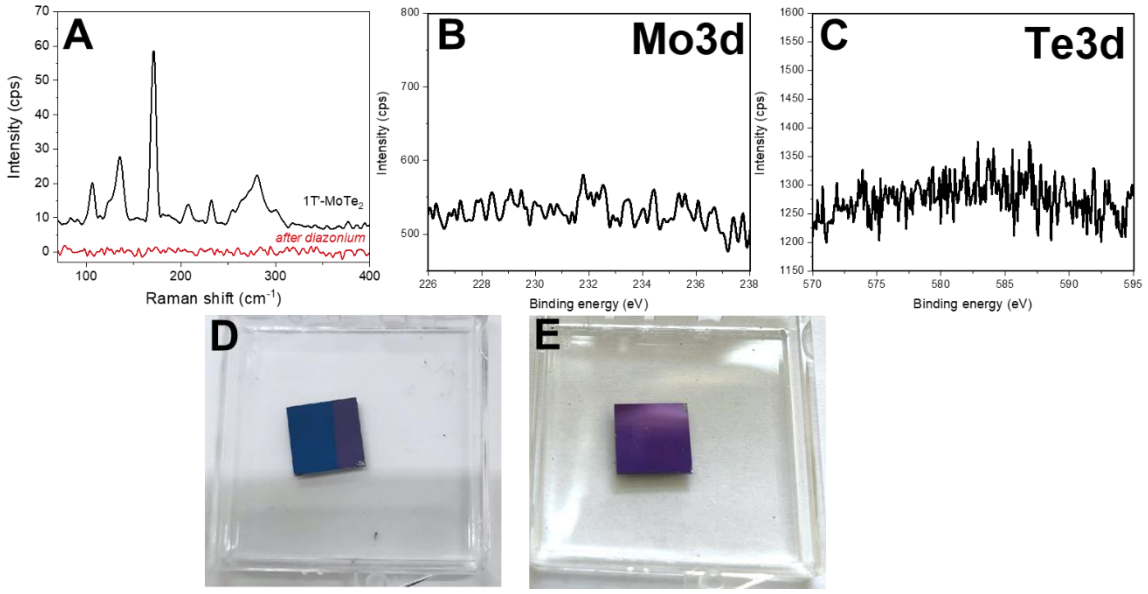

Figure S13. Raman spectra of 1T'-$MoTe_2$ functionalized using DS-CF_3 (measured with 532 nm) (**A**) and corresponding high resolution XPS spectra of Mo 3d (**B**) and Te 3d (**C**) regions, (**D**) - photo of 1T'-$MoTe_2$ before and (**E**) - after functionalization using DS-CF_3

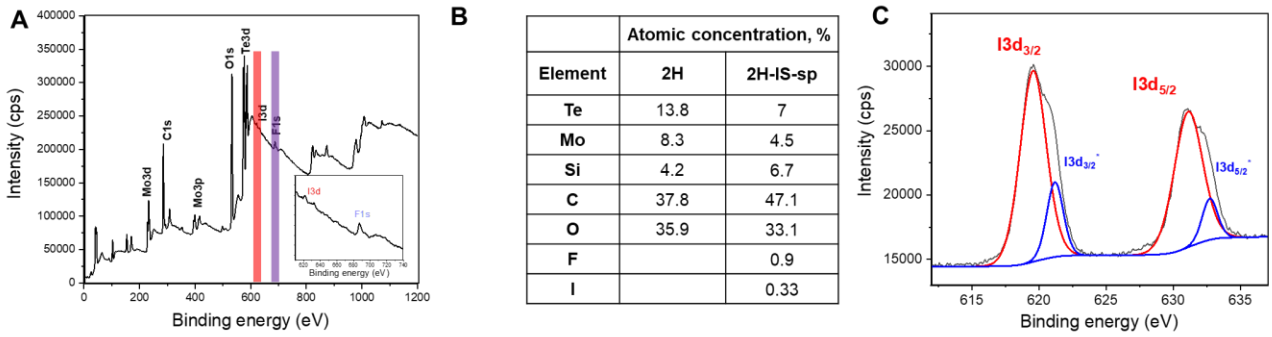

Element	Atomic concentration, %	
	2H	2H-IS-sp
Te	13.8	7
Mo	8.3	4.5
Si	4.2	6.7
C	37.8	47.1
O	35.9	33.1
F		0.9
I		0.33

Figure S14. XPS survey spectrum of 2H-$MoTe_2$ before and after spontaneous treatment with **IS-CF_3** with I 3d and F 1s regions highlighted (**A**); Summary of the atomic percentages for each element present (**B**); High resolution XPS spectrum of the I 3d region (**C**).

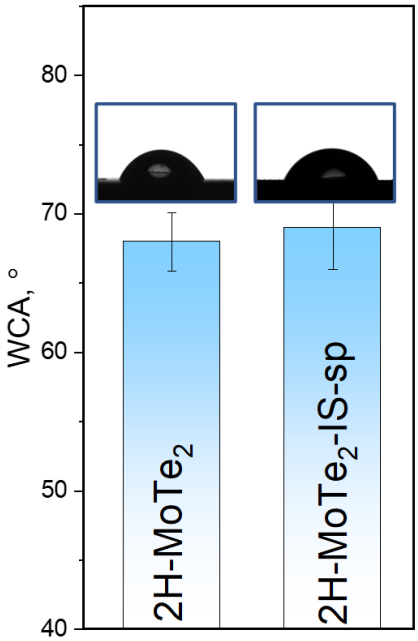

Figure S15. WCA measurements of 2H-$MoTe_2$ before and after IS-CF_3 spontaneous treatment.

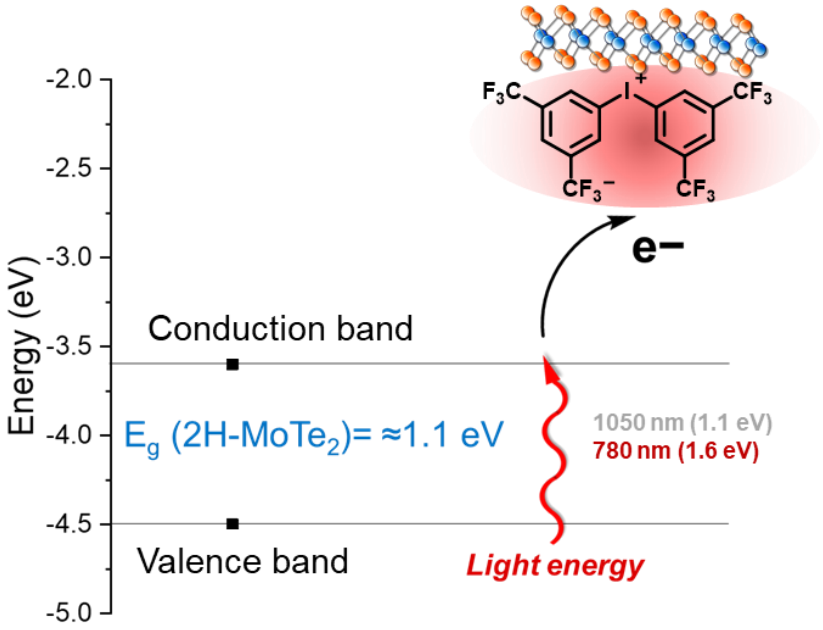

Figure S16. Schematic illustration of light induced electron excitation from 2H-$MoTe_2$.

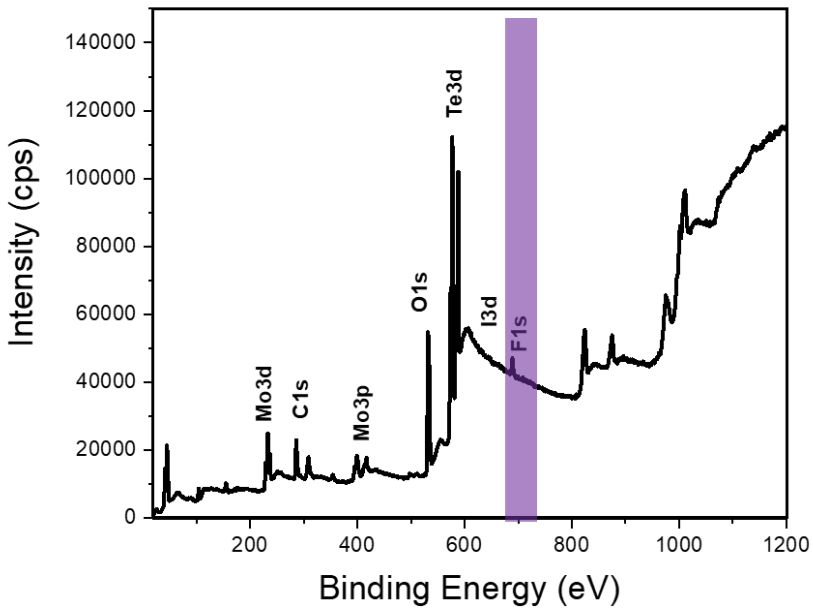

Figure S17. XPS survey spectra of 2H-$MoTe_2$ after interaction with IS-CF_3 under 780 nm light illumination with F 1s region highlighted.

Supplementary Note 3.

Interaction of 2H-$MoTe_2$ with IS-CF_3 under 1050 nm illumination

The energy of the incident photons (*hv*) must be equal to or larger than the band gap (E_g). Thus, we repeated the functionalization reaction of 2H-$MoTe_2$ with **IS-CF_3** under LED light with a 1050 nm wavelength corresponding to energy of ≈ 1.1 eV (Fig. S18A). 2H-$MoTe_2$ films were immersed in the 1mM solution of **IS-CF_3** and illuminated for 1 hour followed by rigorous washing procedures as described above. Unfortunately, the preliminary analysis by XPS measurements did not show any evidence for the presence of Ar-CF_3 signal (Fig. S18B) while the I $d_{3/2}$ and I $d_{5/2}$ peaks are clearly visible still suggesting that physisorption of **IS-CF_3** occured (Fig. S18 C,D). Therefore, we concluded that the light energy (corresponding to 1050 nm wavelength) was too low to generate appreciably high-energy state electron – hole pairs capable of decomposing ISs and to stimulate functionalization. This is unsurprising given the few-layered nature of the film that lacks a direct bandgap.[5]

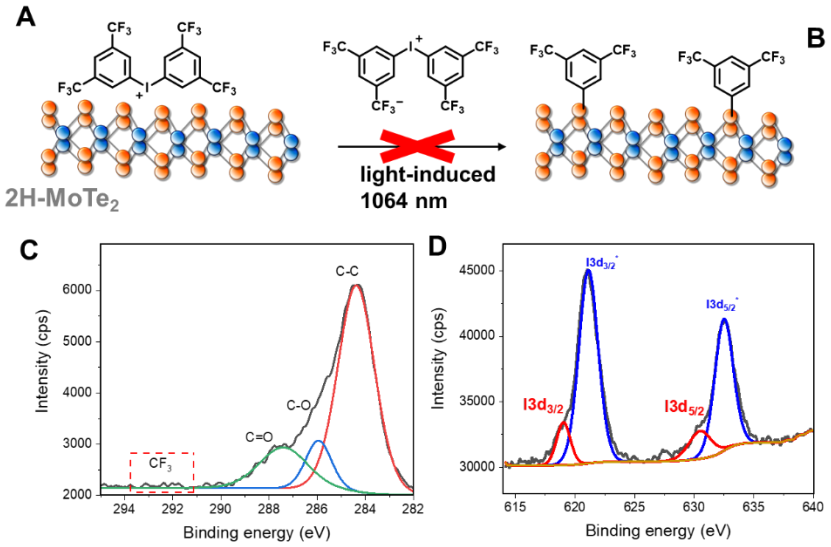

	Atomic concentration, %	
Element	**2H**	**2H-IS-1064 nm**
Te	13.8	11.8
Mo	8.3	7.7
Si	4.2	4.9
C	37.8	41.8
O	35.9	33.2
F		0.82
I		0. 3

Figure S18. Schematic representation of 2H-$MoTe_2$ interaction with IS-CF_3 under 1050 nm light illumination (**A**); Summary of the atomic percentage composition obtained from XPS (**B**); High resolution XPS spectra from the C 1s (**C**) and I 3d regions (**D**).

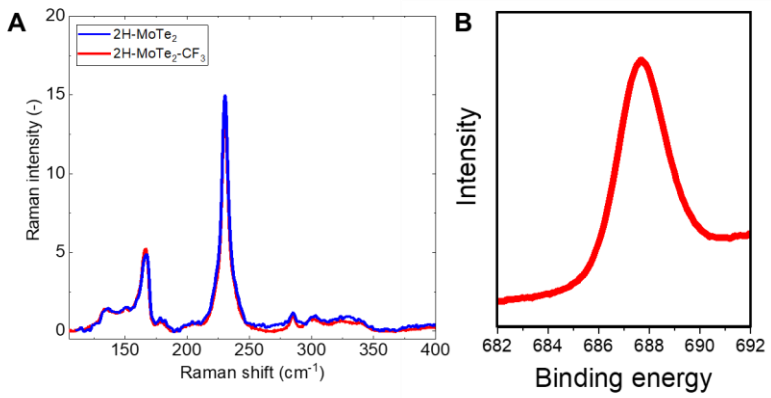

Figure S19. (**A**) Raman spectra (measured at 633 nm) of 2H-$MoTe_2$ before and after interaction with IS-CF_3 under 780 nm light illumination, (**B**) the overlap of all spectra collected on F 1s peak on Fig.3G

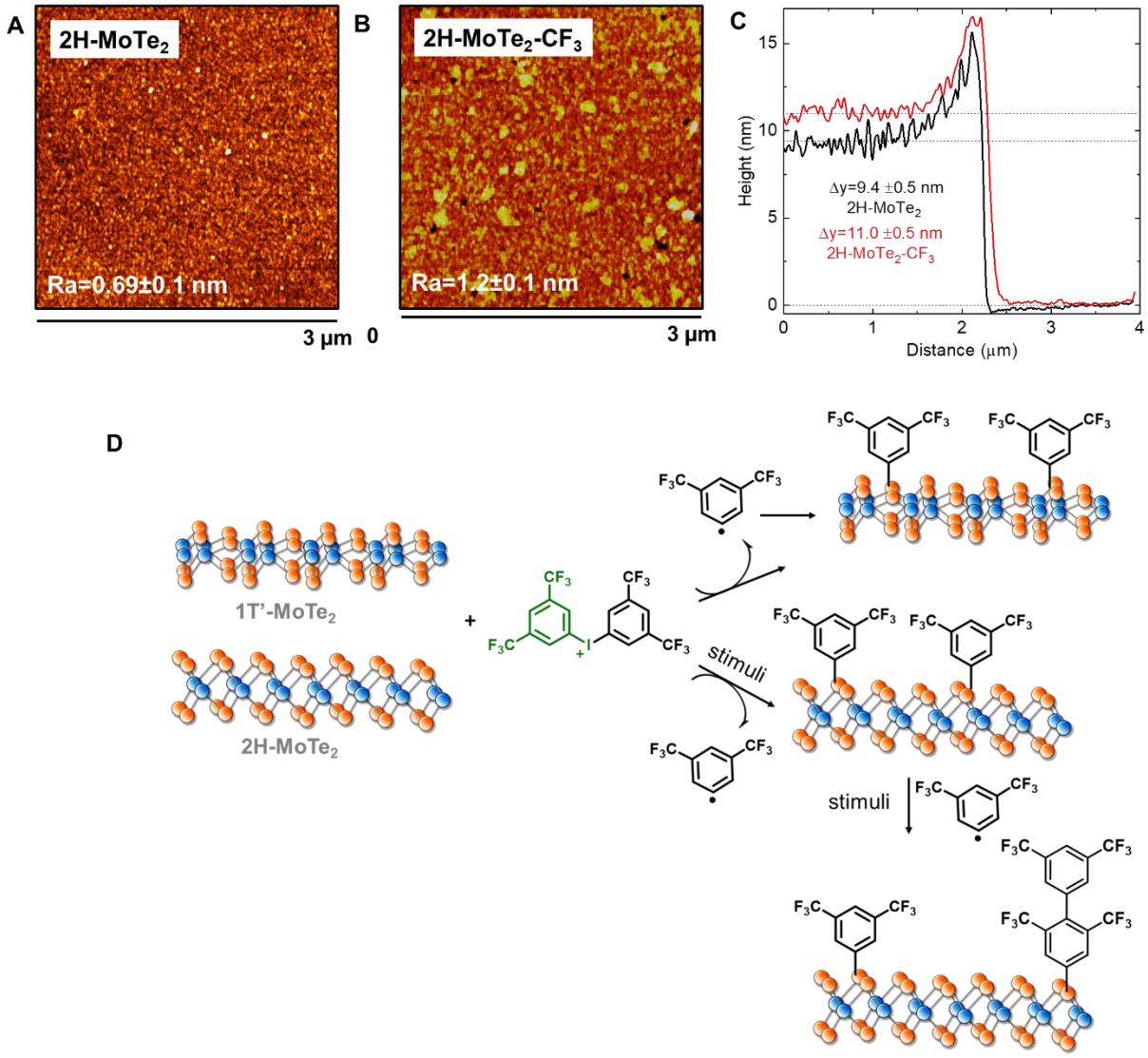

Figure S20. 2D topographical images obtained from 2H-$MoTe_2$ (**A**) and 2H-$MoTe_2$-CF_3 after 780 nm light illumination (**B**) and their corresponding height profiles (**C**). A possible mechanism of functionalization of bilayer formation on 1T- and 2H -MoTe2 films (**D**).

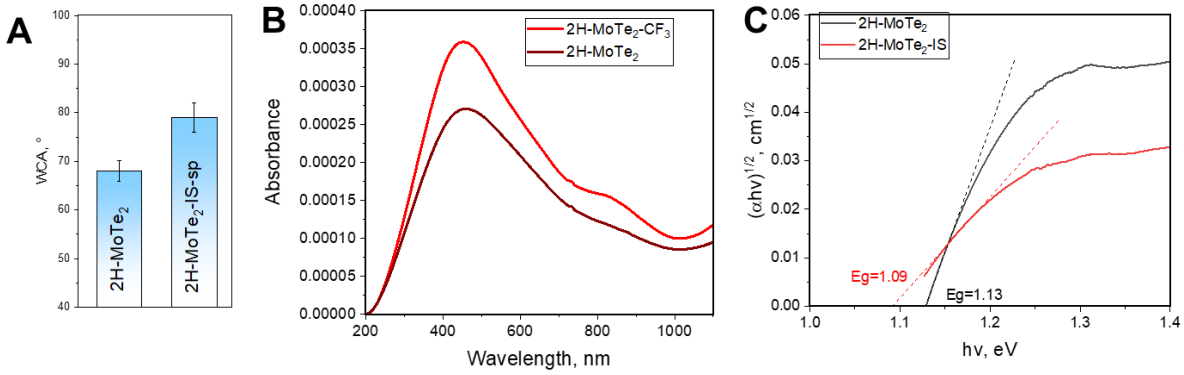

Figure S21. WCA measurements (**A**) and Tauc plot (**B**) for 2H-$MoTe_2$ before and after interaction with IS-CF_3 under 780 nm light illumination

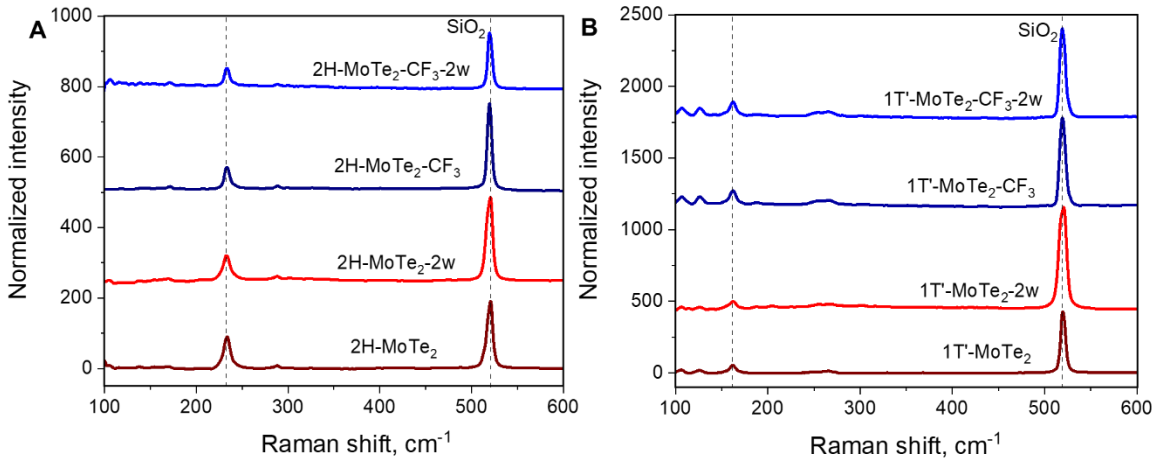

Figure S22. Raman spectra (measured at 532 nm) of pristine $MoTe_2$ and $MoTe_2$-CF_3 for the 2H- (**A**) and 1T'-phases (**B**).

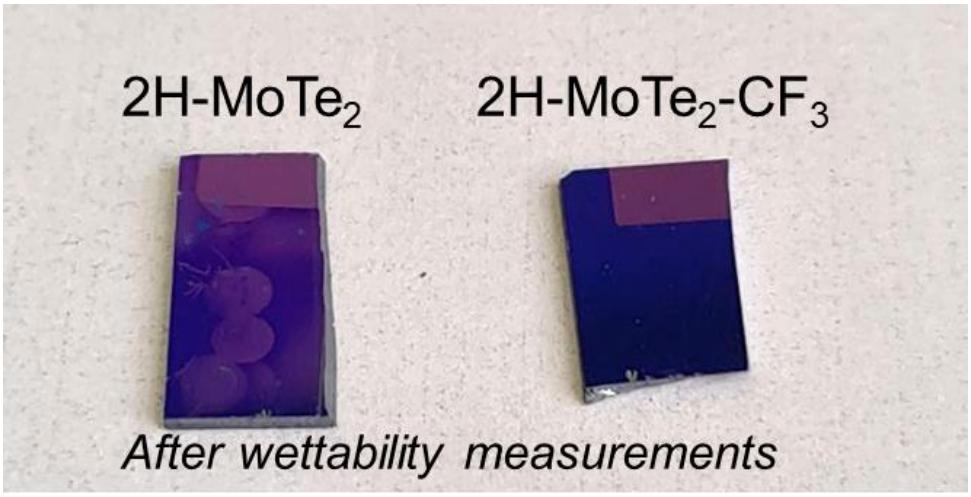

Figure S23. Photos of 2H-$MoTe_2$ and 2H-$MoTe_2$-CF_3 after wettability measurements.

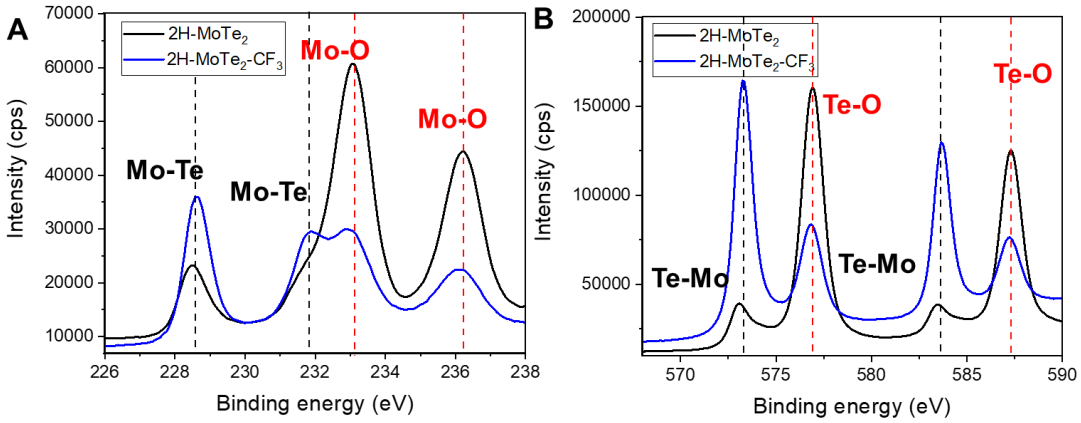

Figure S24. High resolution XPS spectra of the Mo 3d (**A**) and Te 3d (**B**) collected on 2H-$MoTe_2$ and 2H-$MoTe_2$-CF_3 films after water drop deposition.

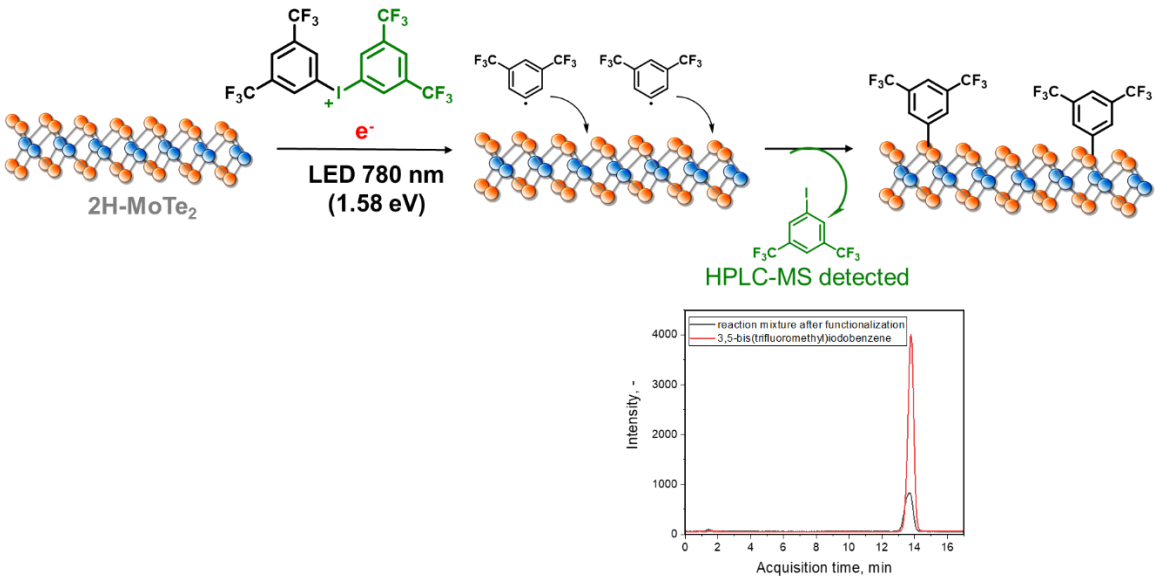

Figure S25. Schematic illustration of the interaction of 2H-$MoTe_2$ with IS-CF_3 under 780 nm light illumination and HPLC-MS chromatogram confirming the presence of 3,5-(trifluoromethyl)iodobenzene.

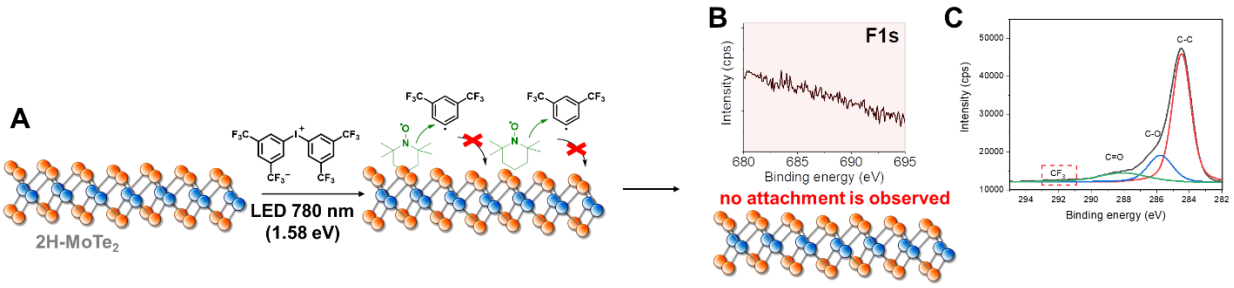

Figure S26. Testing of radical formation during 2H-$MoTe_2$ functionalization (**A**); High resolution XPS spectra from the F 1s (**B**) and C1s regions (**C**) of 2H-$MoTe_2$ after functionalization in the presence of TEMPO.

Additional Synthetic Procedures

Preparation of Bis(3,5-bis(trifluoromethyl)phenyl)iodonium trifluoromethanesulfonate

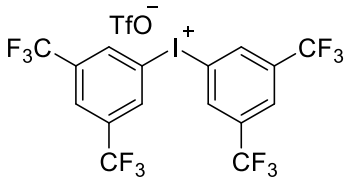

Preparation of IS-$(CF_3)_2$ is based on the previously reported procedure.[9] $NaIO_4$ (3 mmol, 0.642 g) was added to the mixture of trifluoromethanesulfonic acid (10 mL) and iodine (2 mmol, 0.508 g) under argon and stirred at rt for 48 hours. Then the reaction mixture was cooled with in an ice bath and 1,3-bis(trifluoromethyl)benzene (18.2 mmol, 2.8 mL) was added dropwise and the obtained mixture was stirred at ambient temperature for 24 hours. Next, ice was added to the reaction mixture and product was extracted with EtOAc (3×20 ml). Combined organic phases were dried over Na_2SO_4 and solvent was removed in vacuo. The mixture of hexane (10 mL) and Et_2O (2 mL) was added to the residue. The product was filtered off and washed with hexane (3 × 10 mL). Product was dried under vacuo and isolated in 62% yield (3.06 g) as colorless crystalline solid; mp 198–203 °C.^{1}H NMR (400 MHz, Acetone-d_6) δ 9.21 (s, 4H), 8.44 (s, 2H). ^{13}C NMR (100 MHz, Acetone-d_6) δ 137.9 (q, J = 3 Hz), 134.6 (q, J = 34 Hz), 128.0 – 127.7 (m), 123.3 (q, J = 271 Hz), 121.5 (q, J = 318 Hz), 116.4. ^{19}F NMR (376 MHz, Acetone-d_6) δ –63.48, –79.23. HRMS (ESI): m/z calcd. for $[M–TfO^–]^+$ $C_{16}H_6F_{12}I^+$: 552.9322, found 552.9317.

Preparation of 3,5-bis(trifluoromethyl)benzenediazonium tosylate

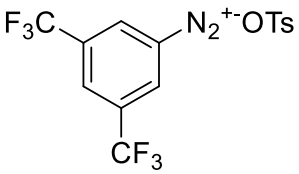

ADT-$(CF_3)_2$ was prepared according to a published procedure.[10] To a solution of p-TsOH (1.425 g, 7.5 mmol) in acetic acid (12 mL), tert-butyl nitrite was slowly added (0.9 mL, 7.5 mmol). Next, 3,5-Bis(trifluoromethyl)aniline (1.15 g, 5 mmol) was added in 4 steps to the reaction mixture over 1 min. The mixture was stirred for 30–40 min until TLC indicated the complete consumption of the amine (hexane/ether 1:1). After completion, the reaction mixture was precipitated by adding diethyl ether (200 mL). The precipitate was washed with diethyl ether, filtered under reduced pressure and dried under vacuum (1.7 g, 78 % yield).

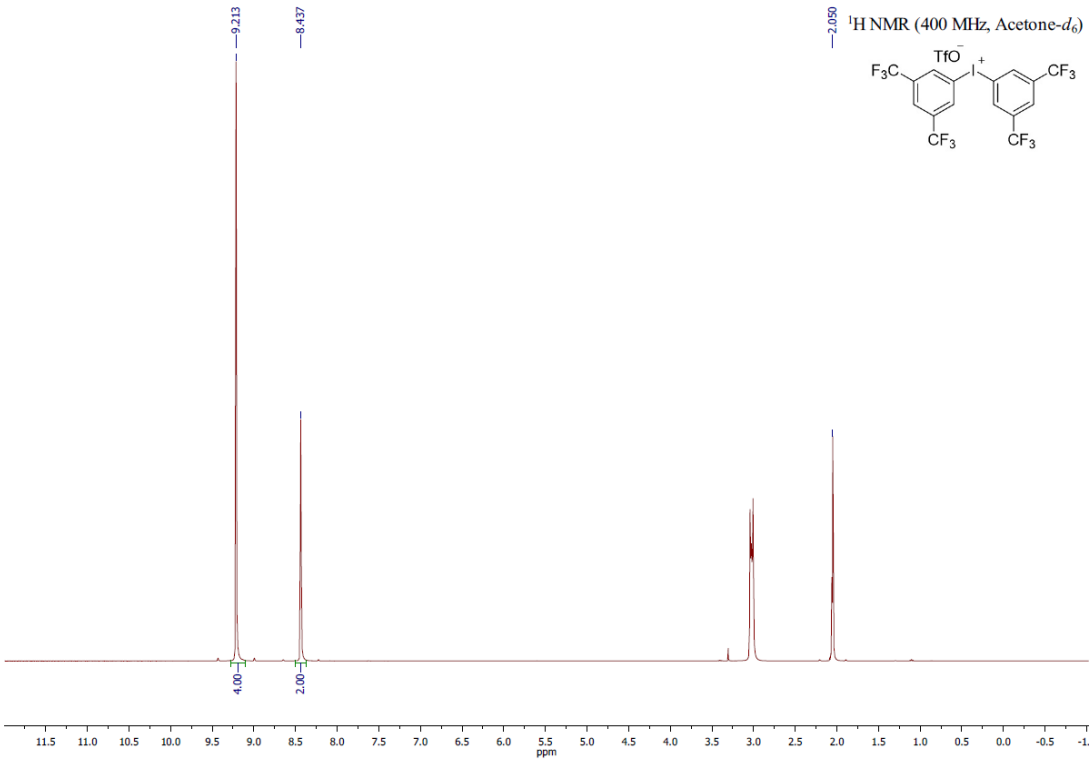

^{1}H NMR (400 MHz, Acetone-d_6)

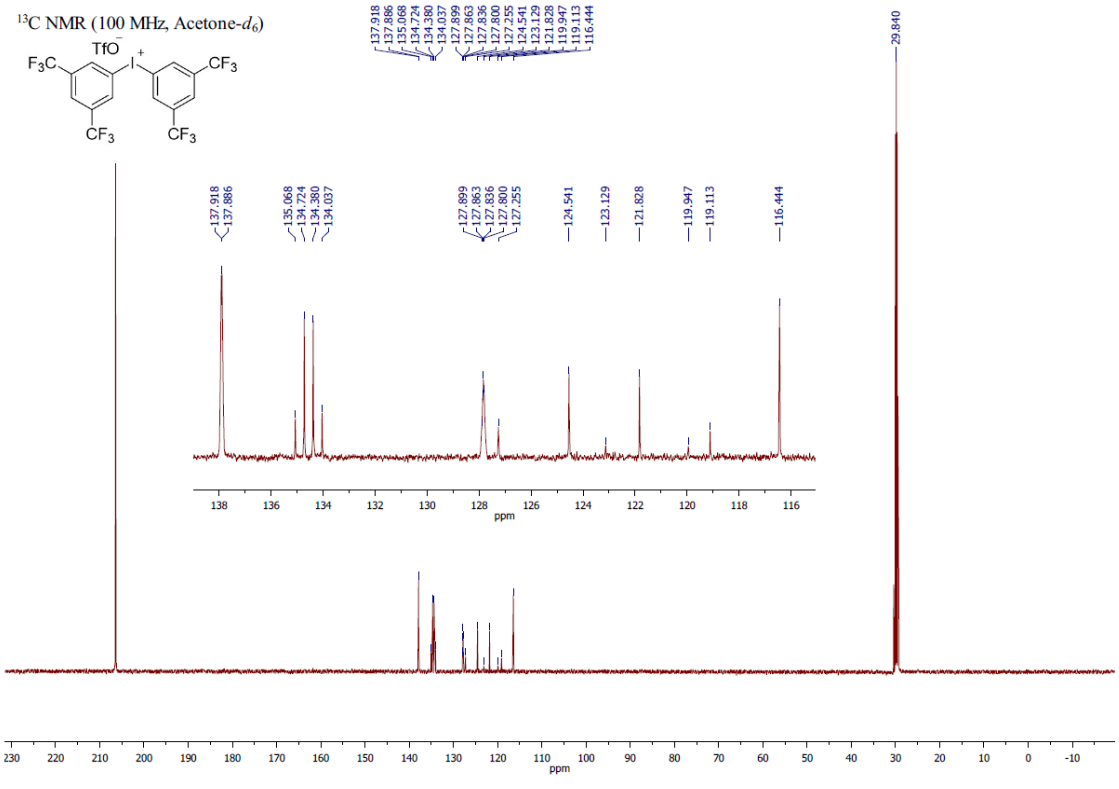

^{13}C NMR (100 MHz, Acetone-d_6)

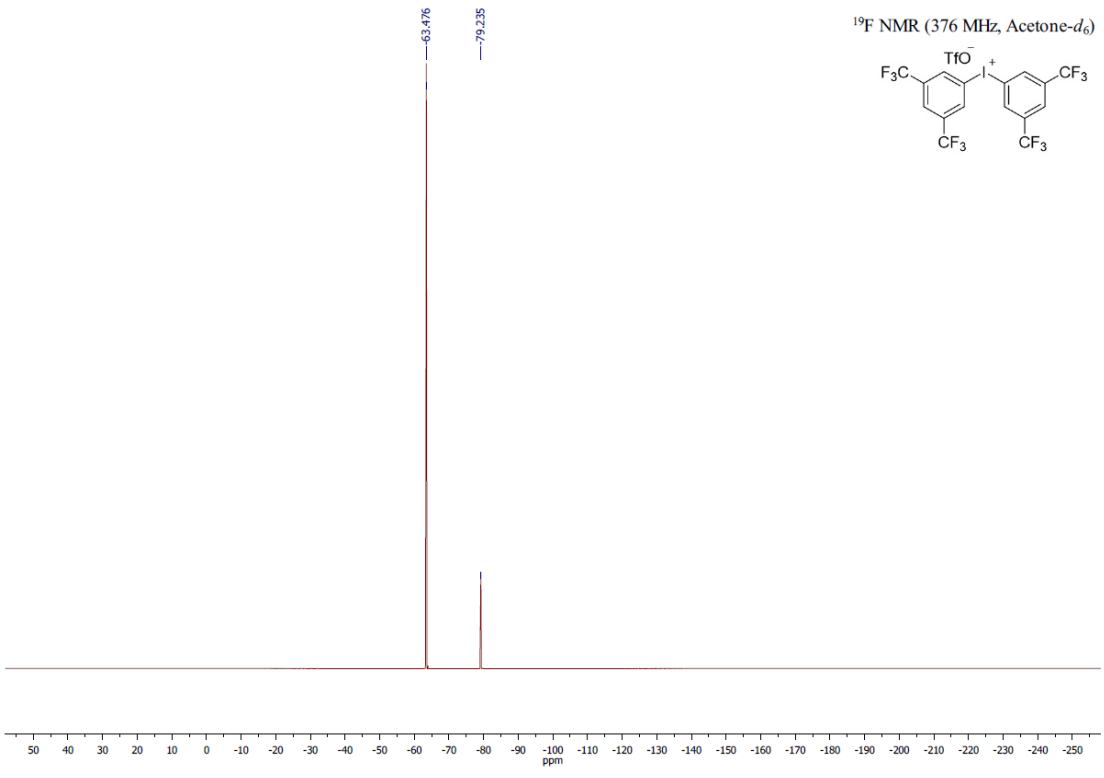

References

1. Yang, L., *et al.*, *Nanoscale* (2018) **10** (42), 19906
2. Gehan, H., *et al.*, *ACS Nano* (2010) **4** (11), 6491
3. Briggs, D. S. M. P., *Practical surface analysis*. Wiley; Salle + Sauerlander: Chichester; New York; Aarau, 1990
4. Wilson, J. A., and Yoffe, A. D., *Advances in Physics* (1969) **18** (73), 193
5. Ruppert, C., *et al.*, *Nano Letters* (2014) **14** (11), 6231
6. Bromley, R. A., *et al.*, *Journal of Physics C: Solid State Physics* (1972) **5** (7), 759
7. Yang, S., *et al.*, *ACS Applied Materials & Interfaces* (2017) **9** (51), 44625
8. Li, D. O., *et al.*, *Molecular Systems Design & Engineering* (2019) **4** (4), 962
9. Dalziel, J. R., *et al.*, *Inorganic Chemistry* (1976) **15** (6), 1247
10. Guselnikova, O., *et al.*, *Separation and Purification Technology* (2020) **240**, 116627